Frequency-Domain Analysis and Design of Thomson-Coil Actuators

Bruno Lequesne, *Life Fellow, IEEE*, Tyler Holp, Steven C. Schmalz, *Member, IEEE*, Robert Michael Slepian, and Hongbin Wang

***Abstract*—Thomson coil actuators consist of an electric coil repelling a metallic disk. They are considered the fastest electromagnetic actuators for short displacements and for this reason are favored for DC circuit breakers. Although the basic physics are understood, the actuator's minimal components are very interdependent, making analysis difficult. Actuator design so far has thus been limited to trial and error based on finite-element models. In this paper, a novel approach is presented based on the electromagnetic frequency response of the actuator. This method is shown to be an intriguing analysis tool and various actuator design directions are presented. Experimental results provide a confirmation of the analysis.**

***Index Terms*—Actuator, circuit breaker, DC breaker, Thomson coil.**

I. Introduction

DC GRIDS are enjoying a renaissance due to the development of renewable energy and the emergence of DC loads such as data centers. The interruption of overcurrent faults is a challenge because unlike AC, the current does not naturally cross zero. Effective DC circuit breakers have thus been identified as key enablers for the future grid [1]. To provide fast interruption with minimal losses at a reasonable price, hybrid configurations have been proposed. An electromechanical actuator breaks the circuit while the current is temporarily diverted [2], [3], [4], [5]. Fast electromechanical actuation is needed however to minimize the stress on the semiconductors through which the fault current is diverted. As a result, Thomson coils are prime candidates for this [5], [6], [7], [8], [9], [10], [11], [12], [13], [14], [15], [16], [17], [18], [19], [20], [21], [22] and are the focus of this paper.

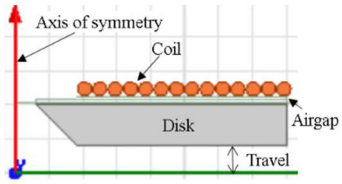

Fig. 1. Thomson-coil actuator.

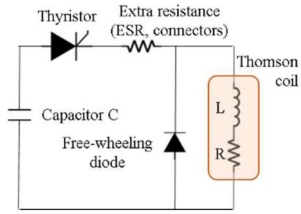

Fig. 2. Thomson-coil circuit.

A Thomson coil actuator is shown schematically in Fig. 1, along with the exciting circuit (Fig. 2). The actuator consists of a coil, which when excited by a current pulse, induces eddy currents in the disk, thus repelling it. The current pulse is generated via discharge of a capacitor triggered by the switching on of the circuit thyristor (Fig. 2).

The basic operation of the actuator has been described before [6], [7]. Early authors developed the relevant mathematical derivations for Thomson-coil actuators, which are quite complex because of the transient aspect and geometrically diffuse nature of the induced currents [6], [7], [9]. The circuit itself is an LCR system, but one where the inductance varies with frequency and disk position. Due to this complexity, some researchers have used experimentation [8], [18]. More recently, designers have relied on finite element analysis (FEA) [9], [11], [15], [16], and even multiphysics [12], [13], [17], [19], [20], the latter in order to include the mechanical aspects of the problem, such as the stress and flexing of the disk [19]. Therefore, the basic physics are known, and engineers have a tool to predict performance.

However, even with such powerful methods, design is still a challenge. The apparatus needs to be reasonably sized, along with energy, voltage, and current levels, leading to an optimization process aimed at getting the fastest motion with the

Manuscript received 8 June 2022; revised 14 September 2022 and 20 November 2022; accepted 24 November 2022. Date of publication 9 January 2023; date of current version 20 March 2023. Paper 2022-EMC-0744.R2, presented at the 2021 IEEE Energy Conversion Congress and Exposition DOI: 10.1109/ECCE47101.2021.9596019, Vancouver, BC Canada, Oct. 10–14, and approved for publication in the IEEE Transactions on Industry Applications by the Electric Machines Committee of the IEEE Industry Applications Society. The information, data, or work presented herein was funded in part by the U.S. Department of Energy Advanced Research Project Agency (ARPA-E), under Award Number DE-AR0001111. *(Corresponding author: Bruno Lequesne.)*

Bruno Lequesne is with E-Motors Consulting, LLC, Menomonee Falls, WI 53051 USA (e-mail: Bruno.lequesne@ieee.org).

Tyler Holp and Robert Michael Slepian are with Circuit Protection Division, Eaton Corp., Moon Twp, PA 15108 USA (e-mail: TylerHolp@eaton.com; MichaelSlepian@eaton.com).

Steven C. Schmalz is with Eaton Research Labs, Menomonee Falls, WI 53051 USA (e-mail: SteveSchmalz@eaton.com).

Hongbin Wang is with Eaton Research Labs, Southfield, MI 48075 USA (e-mail: HongbinWang@eaton.com).

Color versions of one or more figures in this article are available at https://doi.org/10.1109/TIA.2023.3235345.

Digital Object Identifier 10.1109/TIA.2023.3235345

smallest voltage, current, and size possible. While automated optimization is now available [23], a deeper understanding of the factors at play will facilitate reaching a satisfactory trade-off. To this end, this paper proposes a new approach, still using FEA, but based on the frequency response of the actuator instead of the full transient dynamics. This approach provides new insights, including discovery of an electromechanical resonance, and makes it possible to reach a new understanding of design parameter interactions. It is based on a physically sound view of the problem, as corroborated by tests and transient FEA, while making it possible to analyze design parameters independently of one another. The usefulness of the new model resides in both its simplicity and its different outlook on the problem, not emphasizing accuracy, for which transient FEA cannot be surpassed. It is therefore a complement to full transient FEA analysis (not a replacement) as it provides new physical insights as well as faster calculations. As outlined with a few examples, the new method can be used to analyze separately what would otherwise be interdependent design parameters. Being simpler than full transient FEA, it is also much more frugal in terms of computer resources, and could be used for the automated design of Thomson-coil actuators.

Frequency-analysis of non-linear systems is nothing new. However, it is not clear to the authors that it has ever been applied to the analysis of Thomson-coil actuators, or for that matter, limited-motion electromagnetic devices. Such systems operate in a transient state. It is perhaps counter-intuitive to use frequency analysis in such situations, but this paper aims to justify that this is appropriate, owing to a key approximation (also mentioned in [6], [8], [15] for instance). Specifically, the current and the force rise and peak before much motion has occurred, therefore motion can be neglected for the purpose of a simplified analysis.

The paper is organized as follows. A first section describes the system in more details and presents the FEA modeling of an early design. The FEA is then used at various stages of the analysis to justify or corroborate simplifying hypotheses and partial results. Then, the new modeling approach is described. The method is then used to analyze a number of actuator design parameters. Experimental results on a recent prototype are presented, before discussion and conclusion sections.

This approach was presented in an earlier conference paper [24]. This article adds more recent and more comprehensive test results (including a variability and durability test), and adds other results from the new modeling technique.

II. System Description and FEA Model

The target application for the Thomson-coil actuator is a DC circuit breaker, shown schematically in Fig. 3 with the vacuum interrupter on top and the Thomson-coil actuator below. The system also includes a damping mechanism (not shown). (See [21] for a study of damping and latching.) The selection of the vacuum interrupter and design of the damping mechanism are beyond the scope of the paper. From a system perspective, the target is for the breaker to open 6 kV at 1 kA peak with a peak allowable clamping voltage across the breaker of 12 kV. The actuator itself was designed to reach 1 mm travel (out of a total 6 mm) within 0.5 ms [1].

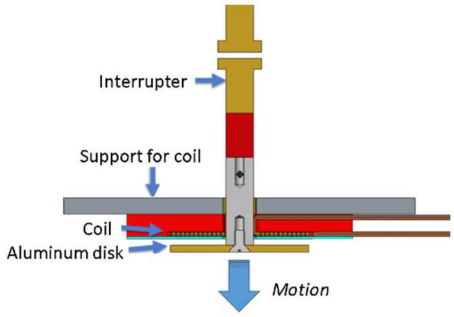

Fig. 3. DC breaker system with Thomson coil actuator.

TABLE I
Thomson-Coil Actuator Prototype Dimensions

Disk	Inner radius	3.2 mm
	Outer radius	38.1 mm
	Thickness	6.0 mm
	Material	Aluminum 6061-T6
Coil	Number of turns	14
	Wire size	12 AWG
	Inner radius	9.3 mm
	Outer radius	38.1 mm
Airgap	Length	0.8 mm
Load	Mass	500 g
Capacitor (electrolytic)	Capacitance	20 mF
	Voltage	275 V

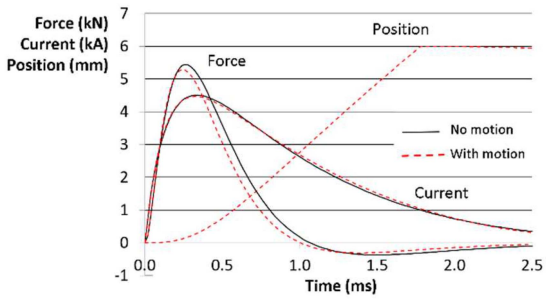

Fig. 4. Force, current, position, with and without motion (FEA).

An initial actuator design was considered for this study. Its dimensions are given in Table I. A load of 500 g was assumed in order to take account of the moving parts of the vacuum interrupter, shaft, and damping mechanism. The disk material is aluminum (alloy 6061-T6) which has an advantage over copper because of the stresses in the disk [15], [19].

The FEA model used the ANSYS Maxwell software for the magnetic problem (Fig. 1), and Simplorer for the excitation circuit (Fig. 2). Thanks to axisymmetry, a 2D model takes full account of the geometry. Fig. 4 shows the results of the full transient analysis. An extra resistance and inductance were added to the circuit (30 mΩ and 3.0 μH), as has been done by others [17]. These correspond to the circuit parasitic resistances and

inductances, such as the capacitor ESR, wires, and connectors, which are significant given the low inductance (3 to 5 μH) and resistance (around 12 mΩ) of the coil itself.

Fig. 4 shows the performance in two cases, one including motion (broken lines) and the other assuming the disk is not moving (solid lines). It is interesting to notice that motion, in fact, has only a small impact on both current and force, even though airgap length affects both inductance and force. The reason is that the current (and thereby force) build-up early in the process, before much motion has taken place. This simplification was used in the past to develop closed-loop formulae [6], [9], and [10], (particularly [6]), but not more recently with the ease of transient FEA analysis. Just the same, the literature on Thomson coil actuators, when motion and current/force are plotted for a given system, consistently shows force and current peaking as motion has barely begun [9], [10], [11], [13], [14], [16], [17], and [20]. Quoting [15], "the variables influencing the rise time of the current pulse … will be dimensioned in such a way as to induce the repulsive forces at low air gaps, i.e., prior to any considerable mechanical movement". Therefore, models without motion are sufficient to estimate current and force profiles. We will make use of this observation in the rest of the paper.

III. System Equations

A. Circuit Equations

The coil drive is an RLC circuit (Fig. 2). The capacitor C holds the energy for the motion. The inductance L is the inductance of the coil (plus that of wiring and capacitor). L varies with frequency and disk position, but as seen above and further shown later, the range for L is relatively small (2 to 1 or so), so as a first step, it is assumed constant. The resistance R is the sum of the inner resistance of the capacitor (ESR), the resistance of the wires and connectors, and of the coil. It is also impacted by frequency, but only at frequencies beyond practical coil designs.

RLC circuit equations are well known. Specifically:

- The initial slope of current I versus time is voltage V over inductance L. Capacitance is not a factor:

$$\left(\frac{dI}{dt}\right)_{time=0} = \frac{V}{L} \tag{1}$$

- The current waveform is critically damped for the following value of R, and underdamped or overdamped if R is below or above this value, respectively:

$$R = 2\sqrt{L/C} \tag{2}$$

- The time for current peak, t_{peak}, is given by:

$$t_{peak} = \varphi/B \tag{3}$$

with, if underdamped: $\tan(\varphi) = \frac{B}{A}$
or if overdamped: $\tanh(\varphi) = \frac{B}{A}$
where: $A = \frac{R}{2L}$ and $B = \sqrt{\frac{|4L - R^2C|}{4L^2\,C}}$

- The maximum value of t_{peak} occurs when R = 0:

$$t_{peak}\ (\max) = \frac{\pi}{2}\sqrt{LC} \tag{4}$$

which corresponds to the minimum frequency f_{min}:

$$f_{\min} = \frac{1}{2\pi\sqrt{LC}} \tag{5}$$

The current therefore starts with the same slope V/L regardless of the resistance and capacitance values. However, the larger the resistance, the earlier and the lower the peak in current. Minimizing the resistance, especially the capacitor ESR, is therefore a critical aspect of an effective design.

B. Force on Thomson-Coil Disk

The repulsion force on the disk is the result of the interplay of the coil current with the current induced in the disk. A number of authors have derived it as a function of the coil current I_{coil}, disk current I_{disk} (induced by the coil current), and the mutual inductance M between the two, the latter in the form of its derivative with respect to displacement x (varying airgap) [10], [11], [19], [25], and [26]:

$$F = I_{coil}\, I_{disk}\, \frac{dM}{dx} \tag{6}$$

For the present purpose, it is useful to consider the case where the coil current is a sinusoidal:

$$I_{coil}(t) = I_{coil} \sin(\omega t) \tag{7}$$

A Thomson coil is essentially a transformer with a single, short-circuited turn (the disk) as its secondary. Based on this analogy, if the coil current is sinusoidal, and with motion neglected, the induced current in the disk is also sinusoidal with a fundamental component at the same frequency and out of phase by some angle φ. Therefore:

$$I_{disk}(t) = I_{disk} \sin(\omega t + \varphi) \tag{8}$$

Again by analogy with transformers, the disk current is proportional to the coil current, by a factor k. k is the turns ratio between the secondary (i.e., the solid disk) and the coil, reduced by the presence of the airgap:

$$I_{disk} = k\, I_{coil} \tag{9}$$

Combining (6)–(9), we get the force F(t):

$$F(t) = k\, I_{coil}^2 \sin(\omega t)\sin(\omega t + \varphi)\, \frac{dM}{dx} \tag{10}$$

which can be decomposed into DC and AC components:

$$F_{DC}(t) = \frac{1}{2} k\, I_{coil}^2 \frac{dM}{dx} \cos(\varphi) \tag{11}$$

$$F_{AC}(t) = -\frac{1}{2}\, k\, I_{coil}^2 \frac{dM}{dx} \cos(2\omega t + \varphi) \tag{12}$$

The following observations can be made: First, the force (both DC and AC components) is proportional to the square of the coil current magnitude. Second, the frequency of the AC force is twice that of the current (explaining why force peaks before current, Fig. 4). Further, the DC component is always smaller than the magnitude of the AC component, by the factor $\cos(\varphi)$, (i.e., the phase lag between the disk and coil currents). Accordingly, under sustained excitation, the repulsion force is negative once per period (this is the case in Fig. 4 after 1 ms).

C. Circuit Pseudo Frequency and Travel Time

It was seen (Fig. 4) that the current and force peak early, and before the desired travel time (0.5 ms). Said differently, if current keeps flowing in the coil near the end of motion, or for that matter afterwards, such late currents and forces are useless (see also [15]). Stating thus that the current should peak at a time t_{ctpk} roughly equal to half the target time T_{tr}, one can derive an approximate target pseudo frequency f_{ps} for the coil current, since t_{ctpk} is 1/4th of the period T_{ct} of the current.

$$t_{ctpk} = \frac{T_{tr}}{2} \tag{13}$$

$$f_{ps} = \frac{1}{T_{ct}} = \frac{1}{4\, t_{ctpk}} = \frac{1}{2\, T_{tr}} \tag{14}$$

The pseudo frequency is related to circuit parameters L, C, and R by (3). This equation, however, does not lend itself to simple derivations. It is therefore convenient to relate the pseudo frequency of the circuit to its ideal frequency f_{LC} in the absence of resistance, with only L and C, given by (5). This ideal frequency will always be less than the circuit pseudo frequency. Assuming a factor of 2 (corroborated later in this paper, Section IV-B-2) yields, from (5):

$$f_{ps} = 2\, f_{LC} = \frac{1}{\pi\sqrt{LC}} \tag{15}$$

By combining (14) with (15), and noting that $\pi^2 \approx 10$, one gets a convenient target value for the product LC as a function of the desired target time:

$$L\,C = 0.4\, T_{tr}^2 \tag{16}$$

This formula appears better suited to the selection of the capacitance value than the capacitance energy $\left(E = \frac{1}{2}\, C\, V^2\right)$.

IV. System Frequency Response: Approach, Results and Comparison With Transient Model

A. Approach and Results

As stated in the introduction, previous authors have followed either one of two paths: Some developed physical equations. In essence, they calculated the mutual inductance as a function of current and position and developed the relationship "k" between disk and coil currents. Others solved the problem via transient FEA. We present now a novel alternative approach, still using FEA, but based on a frequency analysis of the system. This will provide useful insights, some never observed before. In short, it consists of replacing inherently transient equations with a stationary AC problem. This method will highlight the coupling between the electric circuit and the force, that is, between the electrical and mechanical systems.

To this effect, the FEA model of the initial setup was run with an AC current of constant magnitude (an arbitrary 5 kA) or voltage (250 V) at frequencies from 1 Hz to 100 kHz. The resistance and inductance of the coil were derived as well as the force on the plate. The disk was stationary, as justified earlier.

Looking first at the circuit resistance (Fig. 5), it varies little until frequencies on the order of 5 kHz, beyond the practical

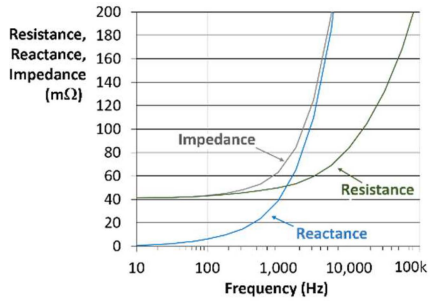

Fig. 5. Resistance, impedance and reactance vs. frequency.

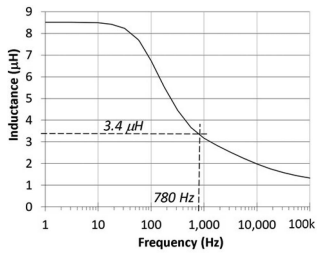

Fig. 6. Inductance vs. frequency (with constant voltage.).

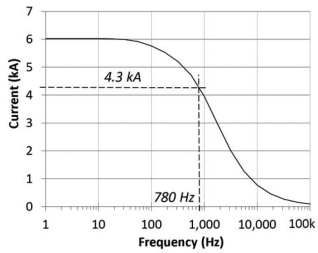

Fig. 7. Current vs. frequency (with constant voltage.).

range for Thomson-coil actuators. The inductance (Fig. 6) on the other hand, is constant at low and high frequencies (8.5 μH and 1 μH, respectively), with a transition between 10 Hz and 10 kHz. At low frequencies, the flux penetrates deep in the disk, providing little reluctance to the flux. At high frequencies, the induced currents in the disk are strong and prevent the magnetic flux from extending beyond the airgap, resulting in a high reluctance. Finally, comparing the resistance, reactance, and impedance of the circuit (Fig. 5), the coil is mostly resistive until around 1 kHz, then largely inductive. As a result, for a constant voltage, the current is constant at low frequencies and drops to essentially zero at higher frequencies (Fig. 7).

The most important result from this analysis, however, is the plot of AC and DC forces versus frequency for a constant voltage (Fig. 8(a)) and constant current (Fig. 8(b)). For a constant voltage, there is a clear resonance taking place in the electromechanical system, with a peak force occurring at a given frequency, around 400 Hz in this case. At low frequencies, little current is induced in the disk, thus no force is produced. As frequency increases, so does the force. At high frequencies, the current in the coil is small due to the high circuit reactance. This drop in

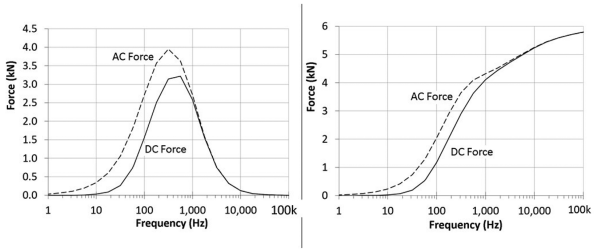

Fig. 8. AC and DC forces vs. frequency, with: (a) Constant voltage. (b) Constant current.

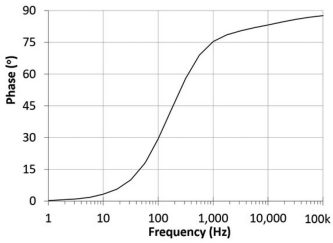

Fig, 9. Phase of AC force relative to coil current.

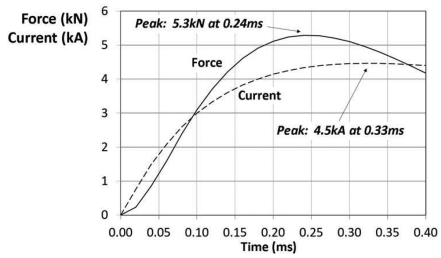

Fig. 10. Transient model: Force and current versus time for exemplary set-up.

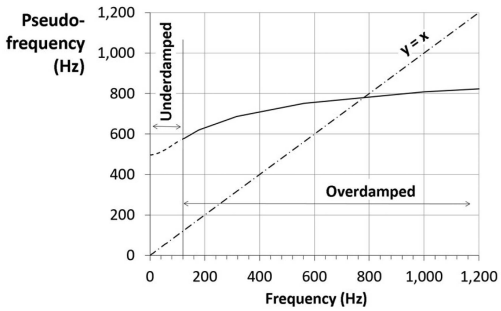

Fig. 11. Graphical solution of (3) for the prototype.

force occurs just below 1 kHz, that is, the frequency at which the circuit goes from resistive to inductive (Fig. 5). If the reactance constraint is removed, the force keeps increasing, as shown in Fig. 8(b) where force is calculated for a constant current. Note also that in both cases (constant voltage or current), the AC force is always equal or larger than the DC force, consistent with (11) and (12). It is equal at low and high frequencies, and larger during resonance.

Continuing on this analysis, Fig. 9 shows the phase of the AC force (phase lag relative to coil current) versus frequency, for a constant current. Based on (12), this is also the phase lag between disk and coil currents. It is similar to the phase shift between primary and secondary currents in a transformer, and goes from 0 to 90°. The transition, between 10 Hz and 1 kHz, matches the resonance of force at a constant voltage (Fig. 8(a)).

The conclusion is that there is a resonance within the electromechanical energy conversion, seen from the bell shape of the force profile. To the authors' knowledge, the existence of such a resonance in the actuator force has not been reported before in the literature. Further, it comes to reason that the force peak could be matched to advantage with the frequency of the electrical circuit.

This novel approach has already provided an interesting new insight into the physics of Thomson-coil actuators by discovering this resonance phenomenon. It can also be used as a complement to the transient FEA model to analyze design parameters (Section V). However, before using the new approach in this manner, in the following section the results of the frequency response analysis (Figs. 5–8) are compared with the more conventional transient FEA model, to ensure that the results from frequency analysis are consistent with actual performance despite simplifying assumptions, most importantly sinusoidal current and effect of motion neglected.

B. Comparing Frequency Response and Transient Model

1) Transient Model: Fig. 10 shows the results of the transient FEA model for the same coil analyzed with frequency analysis, with the addition of motion. "Transient model" refers to the full FEA actuator model versus time, including disk motion, as opposed to the frequency analysis model (Figs. 5–8), which also uses FEA but with stationary excitation. The data in Fig. 10 are the same as in Fig. 4, but with fewer traces and showing only the first 0.4 ms, for clarity.

2) Pseudo Frequency of the Coil Current: The first step in comparing the frequency-model analysis with the transient model is to establish the circuit pseudo frequency from the frequency response. The pseudo frequency is given by (3), with L provided by the frequency response (Fig. 6). This must be solved by iteration, or graphically (Fig. 11). To do so, data for L are obtained for a range of frequencies (as done for Fig. 6). The circuit operating pseudo frequency is calculated versus frequency from (3) for these values of L. The solution is when the calculated pseudo frequency matches the input frequency: In Fig. 11, this is when the result crosses the y = x line.

In this instance, the circuit is underdamped until around 120 Hz (broken trace), then overdamped. The solution is approximately 780 Hz, i.e., a current first peak at 0.32 ms. Referring back to Fig. 10, the transient model shows the current peaks at time 0.33 ms, indicating an excellent match. The frequency analysis assumes operation at a single frequency while the transient model takes into account the full complexity of the dependency of L and R on frequency. The closeness of the two results shows that it is adequate to assume that the system operates at a single frequency (or dominant frequency). Further, this value can be found by frequency analysis alone.

The pseudo frequency is also somewhat less than twice the frequency value when R = 0, which can be similarly calculated to be 425 Hz. This justifies the selection of a factor of 2 leading to (15).

3) Current Peak: The full transient model shows that the current peaks at 4.5 kA (Fig. 10). This value can be compared to the value obtained from the frequency response analysis, shown in Fig. 7. At 780 Hz, the current is around 4.3 kA, very close to the 4.5 kA found in the full transient model. This shows that a frequency response analysis is sufficient to predict both the timing and value of the peak current in the coil. Note that Fig. 7 was calculated for a constant voltage of 250 V. The data in Fig. 10 are for a circuit energized by a capacitor with an initial voltage of 275 V and a voltage reduced at time 0.32 ms to 221 V, such that 250 V is a suitable average value.

4) Inductance: The inductance calculations with the two models can also be compared. The initial slope of current in an LCR circuit is V/L, where V is the initial capacitor voltage (1). The inductance can thus be calculated from Fig. 10 (transient model, initial voltage = 275 V) as 6.65 μH. With an extra circuit inductance of 3 μH, this means the coil inductance is 3.35 μH. Turning to the frequency analysis, the inductance is 3.4 μH at 780 Hz (see Fig. 6), a very close estimate.

5) Force: Fig. 10 also shows the force versus time. It peaks at time 0.24 ms. It is logical to see it peak before the current, since the AC force oscillates at twice the frequency of the current (12). The peak value of the force is 5.3 kN. This is, however, a transient value and a direct correlation with the frequency analysis is more difficult, since that analysis assumes sinusoidal excitation and calculates the DC and AC force separately. Referring to Fig. 8(a), the DC force around 780 Hz is 2.9 kN and the AC force magnitude is 3.1 kN. The transient model result, 5.3 kN, is more than the DC force alone (2.9 kN), and less than the sum of both (6.0 kN).

C. Circuit Pseudo Frequency and Force Resonance

It is important to consider at which frequency the force resonates. As seen in Fig. 8(a), the force peaks (resonates) around 500 Hz (DC force) and 310 Hz (AC force), below the circuit pseudo frequency (780 Hz). If the system were operating at the force resonant frequency, the DC force would be 3.3 kN (14% more than at 780 Hz) and the AC force magnitude would be 3.9 kN (22% more than at 780 Hz). It may thus be that this initial design was close to, but not at, optimum.

V. Actuator Parameter Analysis

A. Method

Frequency analysis makes it possible to analyze Thomson-coil actuators one parameter at a time, thus providing unique physical insights. This is done by analyzing geometries with FEA in Cartesian coordinates, where the disk, which now must be called a plate, is infinitely long and very wide. In doing so, wire spacing, size, shape, airgap, materials, coil size and a number of other design parameters can be analyzed independently of one another. Figs. 12 and 13 illustrate this method for the case of wire spacing. The figures show the two wires and the large plate

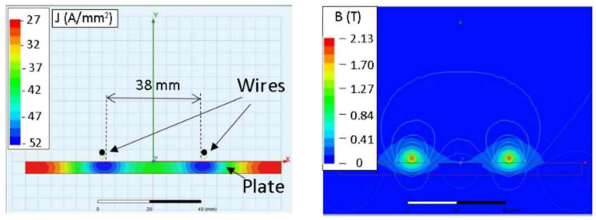

Fig. 12. Model of 2 wires, far apart: (a) Current densities. (b) Flux densities.

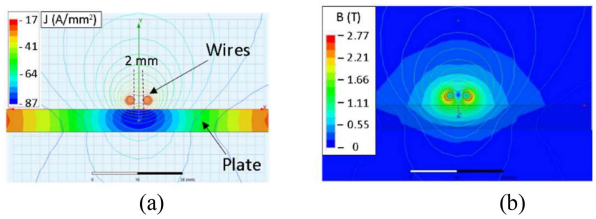

Fig. 13. Model of 2 wires, close together: (a) Current densities. (b) Flux densities. (Both Figs. 12 and 13 shown for 100 V at 60 Hz.).

TABLE II
Dimensions for Thomson Coil Parameter Analysis

Plate	Width	200 mm
	Length	Infinite (2D)
	Thickness	5.0 mm
	Material	Copper
Wires	Diameter	2.0 mm
Airgap	Length	1.0 mm
Excitation	Voltage	100V

across the airgap, with current and flux densities at 60 Hz. This geometry can easily be modeled by FEA to provide the frequency response of the system as a function of a single parameter, wire spacing in this example. Table II provides dimensions used for the analysis.

B. Wire Sacing and Coil Width

These two questions were addressed with the proposed new method in [24]. Briefly summarizing the results:

The wires should be as close to one another as practical.

Force varies linearly with spacing distance when far apart (>10 mm), and with the square of distance when close (<2 mm). When close, as illustrated in Fig. 14, there is a mutual inductance between each wire and the plate current induced not only by this wire, but by its neighbor as well. This cross-coupling does not occur when the wires are far apart.

For the same physical reason, the force goes with the square of coil width when it is small, and linearly with coil width for larger values (beyond 10 mm). For lower coil widths w, less than 10 mm:

$$F_{peak} = \alpha w^2 e^{\lambda w} \; (\lambda = 0.11) \tag{17}$$

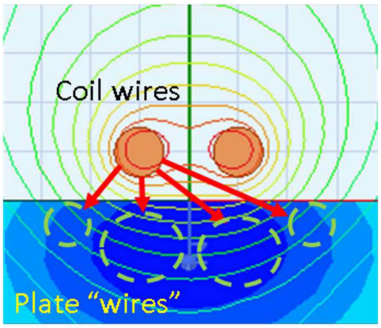

Fig. 14. Current induced by two wires and interaction with plate current; The shades of blue indicate induced currents.

and for larger widths (w > 10 mm):

$$F_{peak} = \beta\,(w+\gamma)\,\left(1-e^{\lambda w}\right)(\lambda = 0.20) \qquad (18)$$

where α, β and γ are constants selected for curve fitting.

C. Number of Turns for Given Coil Width

The selection of the number of turns is a critical design element. The difficulty, usually, consists of separating this question from a number of other ones, such as wire size, disk size, etc. To overcome this limitation, two similar designs, but with one important difference, are now compared. They are based on a given geometry with 16 turns facing a disk, connected as follows: In one case, all in series. In the other case, the turns are divided in two groups of 8, placed in parallel. In order to neutralize the effect of axisymmetry, whereby outer turns are longer than inner turns, the turns are assigned alternately to one group of 8 or the other from the inside to the outside of the coil. It follows that the parallel configuration, in essence, uses exactly half the number of equivalent turns, with everything else being the same.

The results are shown as, first force for a constant voltage (Fig. 15), then for a constant line current (Fig. 16), for which the current is half in each branch for the parallel case. The case with the 16 turns in series is shown on the left and the case of 8 turns in parallel with 8 other turns on the right. The results are direct ratios of one another. For a constant voltage, the force is 4 times larger with 8 turns in parallel with 8 others because the current is twice as large and force goes with the square of current. For a constant overall line current, the opposite is true: The force is 4 times larger in the series case, because there are twice as many effective turns.

The conclusion is if one operates within a current limit, it is better to have as many turns as possible, as this increases the Ampere-turns. Conversely, if there is a voltage limit, fewer turns are better in order to draw as much current as possible. This is because the impedance of the circuit goes with N^2 (N being the number of turns equivalent), therefore for a given voltage, current goes with $1/N^2$ and the Ampere-turns (NI) go with 1/N. These principles can guide actuator design, with the thyristor rating establishing the current limit and the capacitor selection and charging circuit providing the voltage limit.

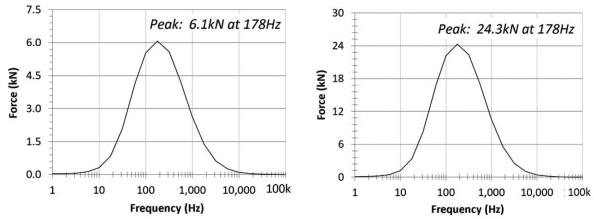

(a) (b)

Fig. 15. Force vs. frequency for constant voltage: (a) 16 turns in series. (b) 8 turns in parallel with 8 other turns.

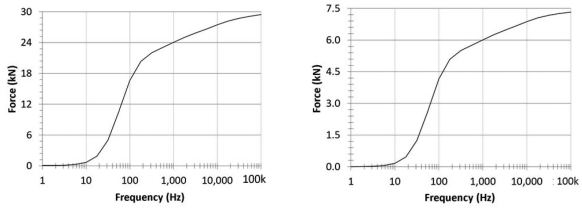

(a) (b)

Fig. 16. Force vs. frequency for constant current: (a) 16 turns in series. (b) 8 turns in parallel with 8 other turns.

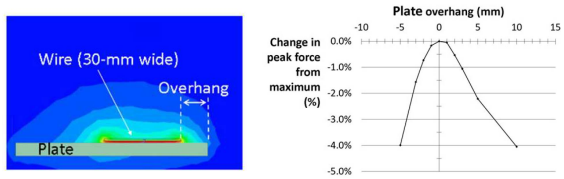

(a) (b)

Fig. 17. Model of plate overhang: (a) FEA plot. (b) Results.

D. End Effects: Coil Width Versus Plate Width

The following addresses the question of whether the coil should be wider than the plate, or vice-versa. The question was answered by analyzing in Cartesian coordinates a single, flat wire facing a plate, keeping the wire width constant and varying the plate's width, see Fig. 17(a). The results are shown in Fig. 17(b), with overhang = 0 denoting a wire (or coil) flush with the plate. Peak force varies remarkably little, with a loss of just 4% in peak force even when the plate is considerably longer (+10 mm) or shorter (−5 mm) than the plate. There is therefore some design latitude in this respect, with the optimum being plate and coil ends aligned with one another (or a shorter plate if plate mass is a factor).

VI. Experiments

A complete DC circuit breaker prototype was built for the target 6 kV/1 kA current interruption, and tested (Fig. 18). Fig. 18 shows the production vacuum interrupter used for the tests (top) and Thomson-coil actuator (bottom), with a zoomed-in window for more details of the actuator. Damping and latching mechanisms (not shown), both beyond the scope of the paper, were also included in the prototype.

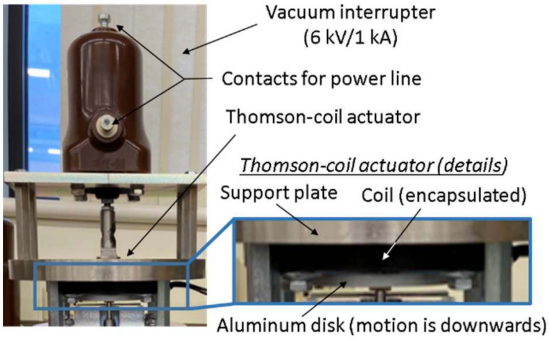

Fig. 18. Picture of the experimental setup.

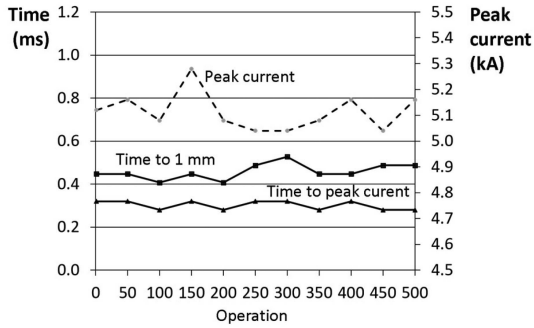

Fig. 20. Test results: Variability over 500 cycles.

TABLE III
THOMSON-COIL ACTUATOR PROTOTYPE DIMENSIONS

Disk	Inner radius	3.3 mm
	Outer radius	38.1 mm
	Thickness	6.0 mm
	Material	Aluminum 6061-T6
Coil	Number of turns	17
	Wire size	14 AWG
	Inner radius	10.3 mm
	Outer radius	38.0 mm
Airgap	Length (including epoxy on coil)	1.6 mm
Load	Mass	504 g
Capacitor (electrolytic)	Capacitance	15 mF
	Voltage	300 V

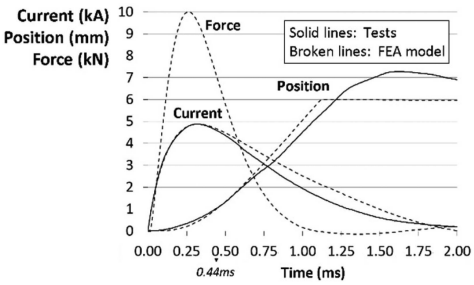

Fig. 19. Prototype test results compared to FEA.

The dimensions for the Thomson-coil actuator (Table III) differ slightly from those used for the above analysis. A 1.6-mm airgap, more practical for production, was used. The coil and capacitors were changed. The moving mass, 504 g as measured, corresponds to the moving parts of the vacuum interrupter, shaft, and damping mechanism.

The test results are compared in Fig. 19 with those obtained from transient FEA. Motion was measured with a laser sensor. The extra resistance and inductance added to the circuit to account for capacitor ESR, wires, connectors, etc, were 10 mΩ and 1.55 μH, respectively. These values were selected to match the current rise and peak values, as in [17]. Test and FEA results match closely until a position of around 3 mm. The prototype included a damping mechanism, while the model had instead a hard stop at 6 mm. Importantly, the prototype reached 1 mm in 0.44 ms in the test, less than the target 0.5 ms. The experimental set up uses a mechanical damping system, as in [21], as opposed to a second coil as sometimes proposed [22]. Aside from reducing the electronics, a mechanical system is advantageous in that it is triggered automatically at some given disk position. By contrast, a second coil is triggered at a fixed time, regardless of actual displacement, unless a position sensor is added.

A subsequent test was conducted to ascertain the overall durability of the overall system (including the contact, vacuum interrupter, etc), and gauge performance variations over time. The system was actuated 500 times, with time to cool down between operations. Fig. 20 shows the time to peak current and the time to 1 mm as measured every 50 operations (solid lines). The time to 1 mm varied from a low value of 0.407ms to a high of 0.527 ms (-11% and $+15\%$ from average of 0.458 ms), showing a very consistent result given the many parameters (friction, springs, actuator airgap, capacitor recharge level) that are bound to experience some variation. The peak current (Fig. 20, broken line) varied over a smaller range yet: from -1.4% to $+3.3\%$ from the average of 5.1 kA.

VII. DISCUSSION: METHOD VALIDATION, REPRESENTATIVITY, AND USEFULNESS

The proposed frequency analysis was validated, first by comparing with full-system, transient FEA, and then by comparing the results with tests. It should be pointed out that the calculations for the frequency analysis use the exact same FEA model as the transient one, except for two differences. One is that the new model neglects motion. This was discussed in Section II. The second difference is that the proposed model uses a stationary AC excitation (one frequency at a time), instead of full transient. It will be recognized however, that if a model can adequately represent full transients and motion (Fig. 19), it will represent a simpler stationary excitation with no motion at least as well.

The analysis in the paper shows that at least for the specific actuator under study, the system exhibits a dominant pseudo-frequency, as opposed to a wide array of frequencies. Therefore, the frequency analysis is a good representation of the system, once the operating frequency is established (as explained in Section IV-B-2). However, even if that was not the case and the capacitor excitation needed to be modeled with a range of frequencies, the frequency-analysis model would still be valid

by using averages of current or force over the expected frequency range. Notably, the resonance seen in Fig. 8(a) would still exist, although the bell shape would be wider and less high. The frequency analysis therefore offers a good representation of the system, including all its design parameters (except of course the circuit elements such as capacitance and voltage). Qualitative conclusions such as those derived in the paper will hold, whether the operating frequency range is narrow or wider.

This said, the new model cannot be as accurate (quantitatively speaking) as a full transient model. Its usefulness resides in two other aspects: (1) rapidity of computer calculations, and perhaps more importantly, (2) in the potential for new analysis resulting from the decoupling of interdependent design parameters (such as, for instance, wire size and coil diameter or number of turns). Concerning the latter, the method has already yielded several findings, most notably the existence of a resonance, relationship between force and distance between wires, etc. These are listed in the conclusion section below. It the authors' hope that the method can be used by others to provide yet finer understandings of Thomson-coil and other limited-motion actuators.

VIII. Conclusion

The paper introduces a novel analysis technique for Thomson-coil actuators. It replaces the transient analysis used before (based on either complex equations or FEA) with a simpler analysis (also FEA based) of the frequency response of the actuator. This perhaps counter-intuitive approach of replacing a transient problem with an analog stationary one, was demonstrated to be valid. Predictions in terms of coil inductance, circuit pseudo-frequency, current magnitude and, to some extent, force level were corroborated by calculations for the full transient system, with the latter being checked against experimental data.

Concerning Thomson-coil actuators, the new method made it possible to draw a number of general conclusions:

- The coil electric circuit operates at one dominant frequency, even though the inductance varies with frequency.
- The circuit operating frequency can be determined from frequency response analysis alone. It is also possible to calculate the peak current from frequency analysis, as well as an approximate value of force.
- The force is a combination of a DC force and an AC force (when excited by a pure sinusoidal current). The frequency of the AC force is twice that of the current. The DC force is slightly less than the magnitude of the AC force, by $\cos\phi$, where ϕ is the phase shift between coil and disk currents.
- It was found that in Thomson-coil actuators, the force for a given voltage resonates at a given frequency. It would be desirable for this frequency to be also that of the coil circuit, or at least to be as close to it as possible.
- It is critical to reduce the circuit resistance as much as possible, especially the parasitic resistance, in order to have the largest current possible.
- Force depends on wire spacing to the square of the distance for small values, and linearly beyond. Similarly, force goes quadratically then linearly, with coil width.
- The number of turns should be selected to balance and maximize the thyristor current and capacitor voltage ratings: more turns for a given current, fewer turns for a given voltage.
- The circuit voltage corresponds to the capacitor rating. The initial current rise is given by the ratio of voltage over total coil-plus-circuit inductance. Then the actual capacitor value can be related to the total inductance and desired travel time T_{tr} by the following formula: $L\,C = 0.4\,T_{tr}^2$. Larger capacitance values only lead to longer, and wasteful, current pulses while smaller values do not take full advantage of the system.

More generally, the paper introduces a novel approach to the study of electromechanical system transients by replacing the transient problem with a simpler one involving the frequency response of the system, which the authors surmise may find useful applications beyond Thomson-coil actuators.

Acknowledgment

The authors are grateful to Messrs. Mahesh Varrier and Arjun Tr of Eaton who provided the initial ANSYS Maxwell model, and to Mr. James Counihan of the Eaton Circuit Protection Division for his assistance with the tests.

References

[1] US Dept. of Energy, "Building reliable electronics to achieve kilovolt effective ratings safely," Dec. 9, 2018. Accessed: Dec. 2, 2022. [Online]. Available: https://arpa-e.energy.gov/technologies/programs/breakers

[2] J.-M. Meyer and A. Rufer, "A DC hybrid circuit breaker with ultra-fast contact opening and integrated gate-commutated thyristors (IGCTs)," *IEEE Trans. Power Del.*, vol. 21, no. 2, pp. 646–651, Apr. 2006, doi: 10.1109/TPWRD.2006.870981.

[3] W. Wen et al., "Research on operating mechanism for ultra-fast 40.5-kV vacuum switches," *IEEE Trans. Power Del.*, vol. 30, no. 6, pp. 2553–2560, Dec. 2015, doi: 10.1109/TPWRD.2015.2409122.

[4] C. Peng, X. Song, A. Q. Huang, and I. Husain, "A medium-voltage hybrid DC circuit breaker—Part II: Ultrafast mechanical switch," *IEEE J. Emerg. Sel. Topics Power Electron.*, vol. 5, no. 1, pp. 289–296, Mar. 2017, doi: 10.1109/JESTPE.2016.2609391.

[5] C. Xu, T. Damle, and L. Graber, "A survey on mechanical switches for hybrid circuit breakers," in *Proc. IEEE Power Energy Soc. Gen. Meeting*, 2019, pp. 1–5, doi: 10.1109/PESGM40551.2019.8973674.

[6] S. Basu and K. D. Srivastava, "Analysis of a fast acting circuit breaker mechanism part I: Electrical aspects," *IEEE Trans. Power App. Syst.*, vol. PAS-91, no. 3, pp. 1197–1203, May 1972, doi: 10.1109/TPAS.1972.293477.

[7] S. Basu and K. D. Srivastava, "Analysis of a fast acting circuit breaker mechanism, part II : Thermal and mechanical aspects," *IEEE Trans. Power App. Syst.*, vol. PAS-91, no. 3, pp. 1203–1211, May 1972, doi: 10.1109/TPAS.1972.293478.

[8] R. J. Rajotte and M. G. Drouet, "Experimental analysis of a fast acting circuit breaker mechanism: Electrical aspects," *IEEE Trans. Power App. Syst.*, vol. 94, no. 1, pp. 89–96, Jan. 1975, doi: 10.1109/T-PAS.1975.31829.

[9] T. Takeuchi, K. Koyama, and M. Tsukima, "Electromagnetic analysis coupled with motion for high-speed circuit breakers of eddy current repulsion using the tableau approach," *Elect. Eng. Jpn.*, vol. 152, no. 4, pp. 8–16, Jul. 2005, doi: https://doi.org/10.1002/eej.20149.

[10] B. Roodenburg, T. Huijser, and B. H. Evenblij, "Simulation of an electro magnetic (EM) drive for a fast opening circuit breaker contact," in *Proc. IEE Pulsed Power Symp.*, 2005, pp. 4/1–4/6, doi: 10.1049/ic:20050033.

[11] Z. Jian, J. Zhuang, C. Wang, J. Wu, and L. Liu, "Simulation analysis and design of a high speed mechanical contact base on electro-magnetic repulsion mechanism," in *Proc. IEEE Int. Conf. Elect. Mach. Syst.*, 2011, pp. 1–5, doi: 10.1109/ICEMS.2011.6073650.

[12] A. Bissal, J. Magnusson, E. Salinas, G. Engdahl, and A. Eriksson, "On the design of ultra-fast electromechanical actuators: A comprehensive multi-physical simulation model," in *Proc. IEEE 6th Int. Conf. Electromagn. Field Problems Appl.*, 2012, pp. 1–4, doi: 10.1109/ICEF.2012.6310320.
[13] A. Bissal, A. Eriksson, J. Magnusson, and G. Engdahl, "Hybrid multi-physics modeling of an ultra-fast electro-mechanical actuator," *Actuators*, vol. 4, no. 4, pp. 314–335, Dec. 2015, doi: 10.3390/act4040314.
[14] V. Puumala and L. Kettunen, "Electromagnetic design of ultrafast electromechanical switches," *IEEE Trans. Power Del.*, vol. 30, no. 3, pp. 1104–1109, Jun. 2015, doi: 10.1109/TPWRD.2014.2362996.
[15] A. Bissal, J. Magnusson, and G. Engdahl, "Electric to mechanical energy conversion of linear ultrafast electromechanical actuators based on stroke requirements," *IEEE Trans. Ind. Appl.*, vol. 51, no. 4, pp. 3059–3067, Jul./Aug. 2015, doi: 10.1109/TIA.2015.2411733.
[16] D. S. Vilchis-Rodriguez, R. Shuttleworth, and M. Barnes, "Finite element analysis and efficiency improvement of the Thomson coil actuator," in *Proc. IEEE 8th IET Int. Conf. Power Electron., Mach. Drives*, 2016, pp. 1–6, doi: 10.1049/cp.2016.0202..
[17] C. Peng, I. Husain, A. Q. Huang, B. Lequesne, and R. Briggs, "A fast mechanical switch for medium-voltage hybrid DC and AC circuit breakers," *IEEE Trans. Ind. Appl.*, vol. 52, no. 4, pp. 2911–2918, Jul./Aug. 2016, doi: 10.1109/TIA.2016.2539122.
[18] C. Peng, "Design, optimization and development of ultra-fast mechanical switch for DC circuit breaker applications," Ph.D. dissertation, EE Dept., North Carolina State Univ., Raleigh, NC, USA, 2016.
[19] D. S. Vilchis-Rodriguez, R. Shuttleworth, and M. Barnes, "Modelling Thomson coils with axis-symmetric problems: Practical accuracy considerations," *IEEE Trans. Energy Convers.*, vol. 32, no. 2, pp. 629–639, Jun. 2017, doi: 10.1109/TEC.2017.2651979.
[20] A. Baudoin et al., "Experimental results from a Thomson-coil actuator for a vacuum interrupter in an HVDC breaker," *J. Eng.*, vol. 2019, no. 17, pp. 3527–3531, 2019, doi: 10.1049/joe.2018.8219.
[21] M.-S. Sim, S. S. H. Bukhari, and J.-S. Ro, "Analysis and design of a Thomson coil actuator system for an HVDC circuit breaker," *IEEE Access*, vol. 10, pp. 58354–58359, 2022, doi: 10.1109/ACCESS.2022.3178724.
[22] T. Augustin, M. Parekh, J. Magnusson, M. Becerra, and H.-P. Nee, "Thomson-coil actuator system for enhanced active resonant DC circuit breakers," *IEEE J. Emerg. Sel. Topics Power Electron.*, vol. 10, no. 1, pp. 800–810, Feb. 2022, doi: 10.1109/JESTPE.2021.3083585.
[23] G. Y. Sizov, P. Zhang, D. M. Ionel, N. A. O. Demerdash, and M. Rosu, "Automated multi-objective design optimization of PM AC machines using computationally efficient FEA and differential evolution," *IEEE Trans. Ind. Appl.*, vol. 49, no. 5, pp. 2086–2096, Sep./Oct. 2013, doi: 10.1109/TIA.2013.2261791.
[24] B. Lequesne, T. Holp, S. Schmalz, M. Slepian, and H. Wang, "Frequency-domain analysis and design of Thomson-coil actuators," in *Proc. IEEE Energy Convers. Congr. Expo.*, 2021, pp. 4081–4088, doi: 10.1109/ECCE47101.2021.9596019.
[25] G. R. Slemon, *Magnetoelectric Devices: Transducers, Transformers and Machines*, Hoboken, NJ, USA: Wiley, 1966.
[26] M. A. Juds, "Thomson coil," in *Practical Magnetic and Electomechanical Design – Solenoids, Actuators, Transformers, Inductors*, Portland, OR, USA: bookbaby.com, 2020, pp. 211–227.

Bruno Lequesne (Life Fellow, IEEE) received the Engineering degree from Centrale-Supélec, Rennes, France, in 1978, and the Ph.D. degree in electrical engineering from the Missouri University of Science and Technology, Rolla, MO, USA, in 1984. He was with General Motors Research Laboratories during 1984–1999, Delphi Research Labs during 1999–2006, and a Group Manager with Delphi Powertrain Division during 2006–2009. After a year with The University of Alabama, Tuscaloosa, AL, USA, he joined Eaton Corporate Research & Technology during 2010–2014. Since 2014, he has been a Consultant with E-Motors Consulting, LLC, Menomonee Falls, WI, USA. He holds 54 patents. He was the recipient of 11 Best Paper Awards, eight from the IEEE- IAS, including two Transactions Awards, and three from the Society of Automotive Engineers. He was elected as an IEEE Fellow in 1997. He was also the recipient of the IEEE IAS Gerald Kliman Innovator Award in 2007 and IEEE Nikola Tesla Award in 2016. He was the past President of the IEEE Industry Applications Society during 2011–2012 and Chair of the IEEE Transportation Electrification Community during 2019–2022.

Tyler Holp received the B.S. degree in mechanical engineering from Pennsylvania State University, State College, PA, USA. From 2013 to 2016, he was a Product Design Engineer working in the new product development of combine harvesters for Deere & Company, Moline, IL, USA. He is currently a Lead Design Engineer working in new product development of medium voltage circuit breakers for Eaton Corporation, Moon Township, PA, USA. His research focuses on fast-acting vacuum switch technology for high-speed interruption in medium voltage circuits.

Steven C. Schmalz (Member, IEEE) the B.S. and M.S. degrees in electrical engineering from Marquette University, Milwaukee, WI, USA. He is currently an Engineering Senior Specialist with Eaton Corporation's Research Labs, Menomonee Falls, WI, USA. He was the Principal Investigator on several research projects funded by the U.S. Government, designing technology for both ground-based and aerospace power applications. He is a licensed Professional Engineer with the State of Wisconsin. He holds 35 patents and trade secrets. In his more than 30 years with Eaton, his principal research interests include sensing technologies, energy management and methods for protecting electrical systems.

Robert Michael Slepian received the B.S.E. degree in engineering science from the University of Michigan, Ann Arbor, MI, USA, in 1975, the M.S. degree in mechanical engineering from Carnegie-Mellon University, Pittsburgh, PA, USA, in 1979, and D.Sc. degree in mechanical engineering from Massachusetts Institute of Technology, Cambridge, MA, USA, in 1984. He was with Westinghouse Research and Development Center from 1975 to 1979 and 1984 to 1996. Since 1994, he has been working for Eaton Electric at their Technology Center in Moon Township, Pennsylvania, where he is currently an Engineering Specialist engaged in design and modeling of circuit breakers. His most recent work involves hybrid circuit breakers which combine conventional current paths with electronic current interruption.

Hongbin Wang received the B.S. and M.S. degrees in mechanical engineering from Xi'an Jiaotong University, Xi'an, China, and the Ph.D. degree from The University of Alabama, Tuscaloosa, AL, USA. He started his career as a Senior Engineer working in new product development of advanced packaging for STMicroelectronics. He is currently a Senior Engineering Specialist working on advanced electromagnetics and cooling technologies for Eaton Corporation's Research Labs, Southfield, MI, USA. His research focuses on the fast and efficient actuation technology for industrial and electrical applications.